






Decline of an ecotone forest: 50 years of demography in the southern boreal forest

JOSEPH D. BIRCH ^{1,†} JAMES A. LUTZ ² E. H. HOGG ³ SUZANNE W. SIMARD,⁴ RICK PELLETIER ¹,
GEORGE H. LAROI,⁵ AND JUSTINE KARST ¹

¹Department of Renewable Resources, University of Alberta, Edmonton, Alberta, Canada

²Department of Wildland Resources, Utah State University, Utah, USA

³Forestry Centre, Canadian Forest Service, Edmonton, Alberta, Canada

⁴Department of Forest and Conservation Sciences, University of British Columbia, Vancouver, British Columbia, Canada

⁵Edmonton, Alberta, Canada

Citation: Birch, J. D., J. A. Lutz, E. H. Hogg, S. W. Simard, R. Pelletier, G. H. LaRoi, and J. Karst. 2019. Decline of an ecotone forest: 50 years of demography in the southern boreal forest. *Ecosphere* 10(4):e02698. 10.1002/ecs2.2698

Abstract. Variation in tree recruitment, mortality, and growth can alter forest community composition and structure. Because tree recruitment and mortality events are generally infrequent, long-time scales are needed to confirm trends in forests. We performed a 50-yr demographic census of a forest plot located on the southern edge of the Canadian boreal forest, a region currently experiencing forest die-back in response to direct and indirect effects of recent severe droughts. Here, we show that over the last 30 yr biomass, basal area, growth, and recruitment have decreased along with a precipitous rise in mortality across the dominant tree species. The stand experienced periods of drought in combination with multiple outbreaks of forest tent caterpillar (*Malacosoma disstria*) and bark beetles. These insect disturbances interacted to increase mortality rates within the stand and decrease stand density. The interaction of endogenous and exogenous factors may shift forests in this region onto novel successional trajectories with the possibility of changes in regional vegetation type.

Key words: aspen; bark beetle; boreal forest; climate response, ecotone; forest demography; long-term plot; *Picea glauca*; *Populus tremuloides*; white spruce.

Received 26 February 2019; accepted 4 March 2019. Corresponding Editor: Debra P. C. Peters.

Copyright: © 2019 The Authors. This is an open access article under the terms of the Creative Commons Attribution License, which permits use, distribution and reproduction in any medium, provided the original work is properly cited.

† **E-mail:** jcooper@ualberta.ca

INTRODUCTION

Forests change through mortality, recruitment of new stems, and growth. These processes underlie stand demography and are critical for predicting the responses to future climates (Kobe 1996, Dietze and Moorcroft 2011, Chen and Luo 2015). Tree mortality rates have increased in forests across North America (van Mantgem et al. 2009, Peng et al. 2011) with some regions demonstrating concomitant reductions in growth and recruitment rates (Barber et al. 2000, Chen and Luo 2015, Hogg et al. 2017). Long-term studies are critical for predicting forest responses to

future climates and disturbance regimes. Of particular importance is to understand how forests have already responded to altered climate to better predict future forest change.

We expect pronounced changes in forest structure and composition at ecotones and especially in northern latitudes. Portions of the boreal forest have already responded to drought with altered demographic rates, shifts in disturbance regimes, and range shifts of some tree species (Soja et al. 2007, Allen et al. 2010). Widespread increases in tree mortality have been reported, particularly for *Populus tremuloides* Michx. in the aspen parkland ecozone that forms an ecotone between the

Great Plains and the boreal forest. In recent decades, *Populus* has experienced drought and insect-induced mortality (Hogg et al. 2002a, Michaelian et al. 2011); however, the decline in tree health is not isolated to *Populus*. *Picea glauca* (Moench) Voss has also experienced drought-induced decline in growth rates across west-central Canada and has projected loss in cover under future climates (Gray and Hamann 2011, Hogg et al. 2017). Mortality rates have risen across the North American boreal forest in the last half-century, and climatic conditions are implicated as the likely driver (Peng et al. 2011, Worrall et al. 2013). As mortality events have become more frequent, a consistent loss in aboveground biomass has arisen across the western boreal forest (Michaelian et al. 2011, Chen and Luo 2015). Continued warming and drying of the southern boreal forest could shift the aspen parkland northward (Hogg and Hurdle 1995, Frelich and Reich 2010). The shift from boreal forest to sparse woodland could be rapid and characteristic of a stable state change (Scheffer et al. 2012). Succession in the western boreal forest is variable but is usually characterized by a transition from *Populus* or *Pinus* or to the more shade-tolerant *Picea* (Brassard and Chen 2006, Bergeron et al. 2014). However, successional pathways could change with future climates and under novel disturbance regimes. As warming and species-specific die-offs within the southern boreal forest continue, understanding stand dynamics and climate responses is crucial to understanding future forest ecosystem processes (Hogg and Hurdle 1995, Hogg et al. 2002a, Michaelian et al. 2011).

To explore how demographic rates changed in the southern boreal forest ecotone, we conducted a 50-yr demographic and tree-ring analysis in a mixed-wood plot situated at the southern edge of the southwestern Canadian boreal forest. Over the past 50 yr, this forest has experienced episodic severe drought, defoliation by forest tent caterpillar (*Malacosoma disstria*), and the and outbreaks of unidentified bark beetles. We compiled and extended the decadal surveys to investigate how demographic rates changed for common tree species and the successional pathway of the forest. Our study provides an unparalleled reference on trends in forest demography in the region to which subsequent studies can be

compared. Importantly, this will allow us to identify deviations from long-term trends in forest structure and composition.

METHODS

Site description

The George LaRoi Forest Plot (herein referred to as the “GLR plot”) covers 1.4 ha (110 × 130 m) of boreal mixed-wood located at 53.408 N, –113.751 W, near Edmonton, Alberta, Canada. The study area is a mixed forest consisting of *Picea glauca* (Moench) Voss, *Pinus banksiana* Lambert, *Populus tremuloides* Michx, and *Betula papyrifera* Marshall, Arbust. The forest exists in one of the southernmost pockets of *Pinus banksiana* within Alberta. Other tree and shrub species in the study area are *Picea mariana* (Miller) Britton, *Prunus virginiana* Linnaeus, *Prunus pensylvanica* Linnaeus f, *Amelanchier alnifolia* (Nuttall) Nuttall ex M. Roemer, *Corylus cornuta* Marshall, and *Salix* spp (Appendix S1: Image S1:S3). Shrub cover is sporadic and aggregated within the plot. The forest originated from natural regeneration in 1925. Burn scars on the oldest snags suggest a stand-replacing wildfire in the early 1920s. The plot has a 20–60 m buffer of forest separating the boundary from adjacent ornamental gardens and private forested land. The soil of the plot is a Brunisol and derived from aeolian parent material. The soil texture is a sandy loam graduating to a loamy sand with increasing depth. The local climate is characterized by a mean annual temperature of $2.2^{\circ} \pm 1.1^{\circ}\text{C}$ (SD), yearly precipitation of 451 ± 78 (SD) mm, and growing season-dominated precipitation of 318 ± 76 (SD) mm (May–September) (Environment and Climate Change Canada 2017). Botanical nomenclature follows Flora of North America (Flora of North America Editorial Committee 1993).

Stand census and stem mapping

The first forest census and stem mapping of the GLR plot was conducted in 1967 as an ecological celebration of Canada’s centennial followed by subsequent censuses in 1977, 1988, 1997, and 2017. The planned 2007 census was not conducted because of insufficient funding. During each census, stems were mapped, and diameter measured to calculate stand density, vital rates (mortality and recruitment), and growth

(basal area increment). The diameter of all tree stems was measured at 1.35 m in height (dbh) to the nearest 0.1 cm. Stems <5.0 cm dbh were measured using calipers and larger trees, using fiberglass dbh tapes. Stems were mapped using mirror compasses and transect tapes. Tapes were stretched along 5 × 5 m quadrats along an N–S orientation, and the perpendicular intersection with a stem was located on the transect. Stems were marked as gone if they were missed in all subsequent surveys (1977–1997), or if no snag or stump was visible in the 2017 survey.

Stand demography

Using census data from across the five decades, we calculated stand and species-level density (stems/ha), mortality and recruitment rates (annually compounded rate), growth (cm/decade), standing biomass (Mg/ha), and basal area (m²/ha). Mortality rates were calculated using an exponential curve; $t_2 - i = t_1 e^{x \times z}$, where t_1 is the abundance at time one, t_2 the abundance at time two, i is recruitment, x the annual compounded rate of change, and z the time in years between time one and two. Recruitment was reported as the total number of stems (alive and recently dead) that grew to 1.35 m in height between censuses. Recruitment annual rates were calculated using an exponential curve; $t_1 + i = t_1 e^{x \times z}$, where t_1 is the abundance at time one, i is recruitment, x the annual compounded rate of change, and z the time in years between time one and two. A stem was classified as recruited if it had not been measured in any previous census and was smaller than 8.0 cm dbh in 2017, due to the 20-yr gap. The 8.0-cm cut-off was derived from the maximum decadal growth observed in stems within the plot. Stems above 8.0 cm were assumed to have been overlooked in previous censuses. Stems of *Picea* and *Pinus* were examined for beetle entry–exit holes and beetle galleries indicative bark beetles. Bark beetle galleries on *Picea* were likely created by multiple species of bark beetle, while those present on *Pinus* were indicative of *Dendroctonus ponderosae*.

Tree biomass estimates were calculated by using allometric equations generated from Canadian-wide data (Ung et al. 2008) and scaled up to the stand by summing all living stems biomass. Summary statistics and graphing of

demographic rates were conducted in the statistical program R version 3.5.0 (R Core Team 2018). The distributions of dbh for living and dead stems were non-normal. A Wilcoxon Rank Sum test was used to test for significant differences between living and dead dbh for each species per census.

Increment core and basal area increment

In May 2017, to calculate annual growth, identify insect disturbances, and reconstruct climate responses, increment cores were taken from a representative subsample of each of the four common tree species; *Picea*; $n = 25$, *Populus*; $n = 18$, *Betula*; $n = 12$, and *Pinus*; $n = 22$. Trees were randomly selected from trees ≥ 10 cm dbh to avoid long-term damage to the tree. Sample size was reduced for *Populus* and *Betula* due to unidentified rot. Two increment cores were taken per tree with a 4.3 mm increment borer (Haglöf Sweden, Mora, Sweden). Increment cores were mounted and sanded with progressively finer grit sandpaper to 1200 grit. Cores were visually crossdated (Fritts 1976, Stokes and Smiley 1996, Speer 2010) scanned at 1200 DPI using a 630 Pro Photo Scanner (Epson, Long Beach, California, USA) and measured using the program Coorecorder 9.3 (Larsson 2018). Crossdating was verified using the COFECHA program (Holmes 1983) and detrended in the statistical program R, using the dplR 1.6.8 package (Bunn et al. 2017, R Core Team 2018). Cores of *Picea* were assessed from pith to bark for signs of diagnostic traumatic resin ducts (TRD), indicating beetle attack in spruce (DeRose et al. 2017), and cores of *Populus* and *Betula* were visually scanned from pith to bark to identify white discolored rings indicating defoliation events (Hogg et al. 2002b; Appendix S1: Fig. S1A, B). Using raw ring widths, we calculated growth rates (mm²/yr) and standardized ring widths for each species. Basal area increment (BAI) was calculated using the dplR package (Bunn et al. 2017). Standardized ring widths were calculated by detrending the width measurements with a spline. Each core was individually detrended to remove low-frequency variation in raw ring width, including age-related growth trend. Multiple splines were visually assessed for goodness of fit, and a Friedman variable span smoother was selected as the most appropriate spline. Standardized tree ring

widths were used in chronology assembly and climate analysis.

Climate response analysis

To determine which climate variables influenced tree growth, we conducted a seasonal climate correlation analysis. We used species-specific chronologies and conducted Pearson correlation analysis between each species' chronology and the climate variables of interest using the R package, *treeclim* 2.0.0 (Zang and Biondi 2015). Specifically, we used the SEAS-CORR procedure (Meko et al. 2011), which uses Monte Carlo simulations to assess significance of the correlations (Percival and Constantine 2006). The chronology was prewhitened, and a bi-weight robust estimate of the mean was used to minimize the influence of outliers on the chronology (Cook 1985). We chose monthly precipitation, mean maximum temperature, and mean minimum temperature as the climate variables for analysis. Our analysis covered the years 1961–2017: the earliest and last year of complete climatic data, respectively. Historical weather data (1961–2017) were concatenated from two climate reporting stations 16 km from the center of the plot at the Edmonton International Airport, Alberta, Canada (Environment and Climate Change Canada 2017). We specified September as the end of the growing season and used season lengths of 1, 3, 6, 9, and 12 months. Monthly correlations are generated by aggregating variables over the season lengths provided. Seasons of different lengths assess the cumulative effect of monthly climate variables on tree growth. We generated Pearson correlation coefficients for the primary and secondary climatic variables for each species. The secondary climate variables are correlated with the residuals of ring width explained by the primary variable. Pearson correlation coefficients were generated for each combination of climate variables as the primary and secondary variable.

Regional forest comparison

To compare the GLR plot dataset with regional plots, we used publicly available Alberta Biomonitoring Institute (ABMI) data. We selected ABMI plots within 200 km of the GLR plot and subset 5 × 5 m cells that were surveyed within 2015, 2016, or 2017 and had at least one species

in common with the GLR plot (ABMI 2018). We performed a non-metric multidimensional ordination (NMDS) with the subset of ABMI data and an equal number of randomly selected 5 × 5 m cells from the GLR plot based on the basal area of tree species. The analysis was performed using the R packages *ecosdist* 2.0.1 and *vegan* 2.5-2 packages (Goslee and Urban 2007, Oksanen et al. 2018). To compare growth trends between *Picea* within the GLR plot and regional plots, we compared mean raw ring widths from seven local sites and Alberta-wide sites measured by Hogg et al. (2017) against those at the GLR plot. Growth data from *Picea* collected by Hogg et al. (2017) were truncated to 1967–2015 for the analysis as well as growth records from several sites spanning subsets of the full analysis period 1967–2015.

RESULTS

Changes to stand density, basal area, and biomass

All species declined in density 1967–2017. Stand density peaked at 2408 stems/ha in 1967 and declined 76% to a low of 569 stems/ha in 2017. *Picea* increased 16% in density from 1066 stems/ha in 1967 to 1245 stems/ha in 1988 before falling 70% to a low of 376 stems/ha in 2017 (Fig. 1A). *Populus* declined by 89% in density from its peak of 1157 stems/ha in 1967 to 127 stems/ha in 2017 (Fig. 1B). *Betula* declined by 65% in density from a high of 108 stems/ha in 1967 to 37 stems/ha in 2017 (Fig. 1C). *Pinus* declined by 61% from a high of 76 stems/ha in 1967 to 29 stems/ha in 2017 (Fig. 1D). Stand basal area increased from 1967 to 1997; it peaked at 28.2 m²/ha in 1997 before declining 29% to 19.8 m²/ha in 2017. Total stand biomass increased from 64 Mg/ha 1967 to a high of 120 Mg/ha in 1997 before declining 25% to 90 Mg/ha in 2017 (Appendix S1: Fig. S2A, B). All species increased in mean dbh through time and, except for *Betula*, had significant differences between living and dead stem dbh at every census point (Appendix S1: Fig. S3A, D). Annual mean basal area increment fluctuated through time. Specifically, mean basal increment of *Populus* precipitously dropped between 1980 and 1988, which coincided with defoliation by *Malacosoma disstria*. All species declined in growth in

2002, likely due to the severe drought in that year (Fig. 2).

Vital rates

Mortality rates varied by species and showed pronounced changes by decade (Fig. 3A). *Picea* mortality rates remained comparatively low 1967–1997, before rising to 5.9% yr⁻¹ during 1997–2017. *Populus* mortality rates peaked at a

rate of 6.8% yr⁻¹ 1988–1997. *Betula* mortality remained stable through time with the lowest mortality rate of 2.1% yr⁻¹ occurring 1977–1988. *Pinus* mortality increased from 0.98% yr⁻¹ in 1967 to 2.3% yr⁻¹ in 2017 but remained the lowest rate across all species. Recruitment rates were low throughout the duration of the study and declined with time (Fig. 3B). Recruitment rates never exceeded mortality rates except for *Picea*

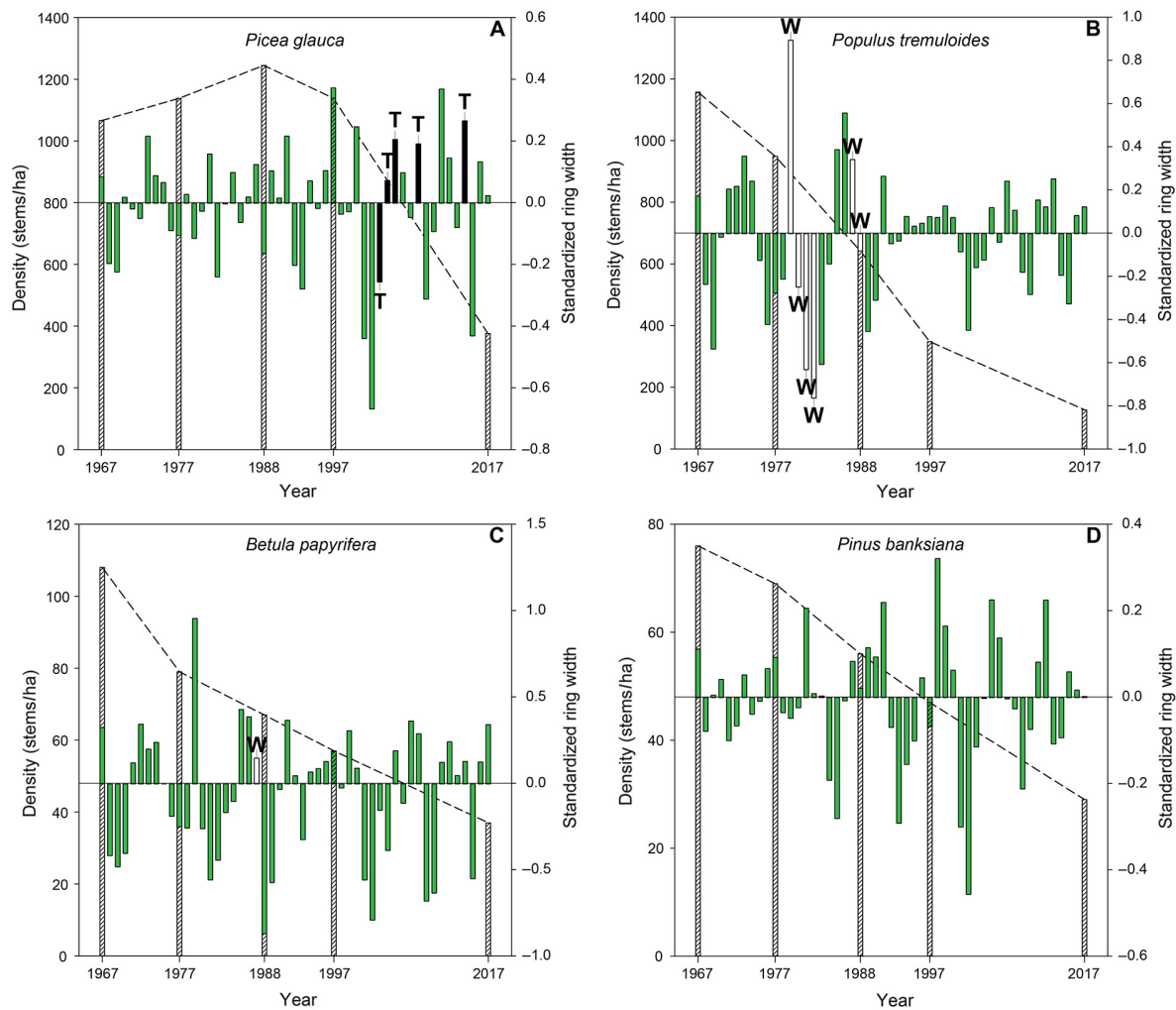


Fig. 1. Tree density (stems/ha; cross-hatched) plotted against standardized ring widths (green) for the George LaRoi forest plot; Alberta, Canada (1967–2017). Tree species are (A) *Picea glauca*; years with traumatic resin ducts in tree rings on $\geq 20\%$ of stems are marked with T and colored black, (B) *Populus tremuloides*; years with white tree rings on $\geq 50\%$ of stems are marked with W, colored white, (C) *Betula papyrifera*; years with white tree rings on 100% of stems are marked with W, colored light gray, and (D) *Pinus banksiana*. Standardized ring widths >0 indicate better-than-average growth with ring widths <0 indicating worse-than-average growth. For visual clarity, the change in tree density for each species is marked by the dashed line.

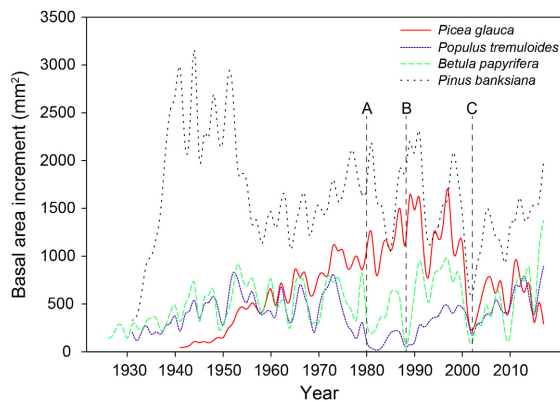


Fig. 2. Mean annual basal area increments for the four common species at the George LaRoi forest plot; Alberta, Canada. Mean rates were averaged across species (*Picea glauca*; $n = 22$; *Populus tremuloides*; $n = 10$; *Betula papyrifera*; $n = 10$; and *Pinus banksiana*; $n = 10$). Rates fluctuated through time and show a precipitous decrease for *Populus* between 1980 (A) and 1988 (B), which corresponds with defoliation by *Malacosoma disstria* (refer to Fig. 1B). All species decreased in growth in 2002 (C), likely due to the severe drought in that year (Fig. 1).

1967–1988. *Picea* recruitment peaked 1977–1988 at an annual rate of $1.6\% \text{ yr}^{-1}$ before decreasing by 79% to $0.35\% \text{ yr}^{-1}$ 1997–2017. *Populus* recruitment declined from a rate of $0.46\% \text{ yr}^{-1}$ in 1967 to $0.13\% \text{ yr}^{-1}$ in 2017. *Betula* recruitment increased from $0.38\% \text{ yr}^{-1}$ from 1967 to 1977 to $1.7\% \text{ yr}^{-1}$ 1988–1997, before falling to $0.69\% \text{ yr}^{-1}$ 1997–2017. *Pinus* recruitment was absent 1967–1997, before rising to $0.07\% \text{ yr}^{-1}$ 1997–2017.

Stand history of insect attack

We observed bands of traumatic resin ducts (TRDs) in *Picea* ($n = 14$) in 11 of 13 yr from 2002 to 2015. The greatest proportion of TRDs was in 2014 with 42% of trees having a TRD (Appendix S1: Fig. S10A). We detected white rings in 100% of cored *Populus* ($n = 18$) and *Betula* ($n = 12$). White rings occurred on *Populus* during 1979–1988. Six of the ten years of white rings had over 50% of the trees affected. The greatest proportion of white rings were detected in 1980 where 100% of *Populus* cores displayed white rings. Interestingly, *Betula* exhibited only one white ring, in 1987, where 100% of individuals show a white ring (Appendix S1: Fig. S10B).

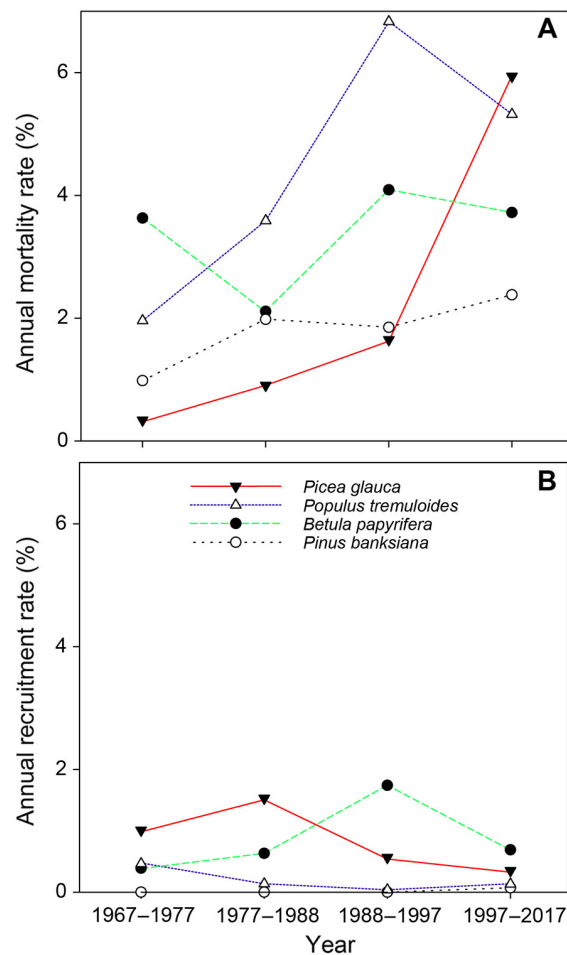


Fig. 3. Average annual mortality (A), and recruitment (B) rates for the George LaRoi forest plot; Alberta, Canada (1967–2017). Closed triangles identify *Picea glauca*, open triangles identify *Populus tremuloides*, closed circles identify *Betula papyrifera*, and open circles identify *Pinus banksiana*.

Diagnostic galleries indicative of mountain pine beetle (*Dendroctonus ponderosae* Hopkins) and *Ips* spp. were observed in less than 20% of *Pinus* individuals ($n \leq 10$). We did not identify any diagnostic features in *Pinus* rings to identify the years of beetle attack. Galleries of multiple species of unidentified bark beetles were observed on *Picea*.

Climate response of trees

Ring widths of all species were significantly correlated with growing season precipitation and declined in annual growth corresponding with

drought. Precipitation and temperature show pronounced variation across years (Appendix S1: Figs. S4A, S5A) and with season (Appendix S1: Figs. S4B, S5B). The highest correlations occurred with precipitation as the primary variable and mean maximum temperature as the secondary variable (Appendix S1: Figs. S6, S9). Of the four species, *Betula* displayed the strongest correlation with precipitation. *Picea* and *Pinus* displayed similar correlations with precipitation but varied in the time of year that was associated with the highest correlation. *Populus* displayed the weakest correlation despite its high sensitivity values (Appendix S1: Table S2).

As season length increased, the strength of correlation increased between monthly precipitation and *Picea* ring growth. June precipitation was the strongest positively correlated variable across all seasons. Mean maximum temperature in the previous year's September was significantly negatively correlated for the 1- and 3-month seasons with November significant at the 6-month season (Appendix S1: Fig. S6). *Picea* growth responded favorably to summer precipitation and negatively to warm fall temperatures of the previous year.

Precipitation was significantly positively correlated with *Populus* growth in the 1-, 3-, 6-, and 9-month seasons. The highest correlation was in the 9-month season in May. The highest overall negative correlation was with mean maximum temperature as a secondary variable in the 6-month season during the previous year's November and December (Appendix S1: Fig. S7). *Populus* growth favors late-spring precipitation and declines with warm wintertime temperatures in the previous year.

The most sensitive species, *Betula*, showed strong positive correlations with precipitation across all season lengths. The highest correlation was with the 9-month season and May and June. Mean maximum temperature was negatively correlated across all seasons and most strongly in the 6-month season during November and December of the previous year (Appendix S1: Fig. S8). *Betula* growth responded favorably with moderately cool, wet conditions, particularly in May and June. As with *Picea* and *Populus*, warm fall and wintertime temperatures are associated with decreased *Betula* growth.

Interestingly, *Pinus* displayed strong, positive correlations with both precipitation and mean maximum temperature. It is the only species to display a positive correlation with mean maximum temperature. The highest correlation with precipitation occurred in the 12-month season in August of the previous year. Mean maximum temperature was most strongly correlated in the 1-month season in December of the previous year (Appendix S1: Fig. S9). The low series inter-correlation and complacency of *Pinus banksiana* resulted in the detection of anomalies in the series due to poorly behaving trees (Appendix S1: Table S2).

Regional forest composition

The GLR plot is statistically similar in composition and raw ring growth to other stands within the region. A NMDS of basal area by species from a random subset of the GLR cells overlapped with ABMI plots within 200 km of the GLR plot (Appendix S1: Fig. S11; ABMI 2018). Additionally, we compared *Picea* raw ring growth from the GLR and that measured by Hogg et al. (2017) for 1967–2015 and found that *Picea* ring growth within the GLR is statistically indistinguishable from provincial growth values in all but two (2003, 2009) of the last 48 yr (Appendix S1: Fig. S12).

DISCUSSION

Our findings detail 50 yr of succession and eventual decline of an ecotone forest undergoing repeated disturbances. The temporal depth and tracking of individual trees through time at the GLR plot provides unique evidence of change at a forest ecotone. Our results highlight dramatic changes in mortality rates, ring growth, and recruitment rates in the last twenty years coinciding with repeated drought and the outbreaks of bark beetles. Cumulatively, the results highlight the deterioration of the original forest cohort and the failure of new cohorts to establish in the fallout of repeated insect disturbance and drought. This has resulted in a new successional trajectory that may become more prevalent in the ecotone with repeated drought and the continued outbreaks of bark beetles and other insects.

Comparison of GLR to regional forests and its departure from historic succession

Mortality rates within the GLR plot have varied over time but display substantial departures from the regional and Canada-wide rates. The 2010 mortality rates for *Picea* are expected to be between 1–2% yr⁻¹ and 2–3% yr⁻¹ for *Populus* (Peng et al. 2011, Zhang et al. 2015). In comparison, we measured 5.94% yr⁻¹ for *Picea* and 5.32% yr⁻¹ for *Populus* 1997–2017 in the GLR plot. Not only are the mortality rates for the GLR elevated above reported values but these mortality rates have grown at double their Canada-wide species-specific rates. Peng et al. (2011) reported that mortality rates are increasing across the Canadian boreal forest with *Picea* increasing by 3.29% yr⁻¹ and *Populus* increasing by 2.84% yr⁻¹. In comparison, the *Picea* mortality rates in GLR increased by 7.1% yr⁻¹ with *Populus* rates increasing by 6.24% yr⁻¹ 1977–1997 and decreasing by 1.24% yr⁻¹ 1997–2017. The average increase in mortality rates for the western Canadian boreal forest was 4.7% yr⁻¹ 1963–2008 (Peng et al. 2011), which is still substantially lower than the rates seen in the GLR plot.

Recruitment rates have largely declined with time for the Canadian boreal forest (Zhang et al. 2015), a trend that we also observed at the GLR plot. The values of recruitment for *Picea* were roughly 20% of expected values in 1977, 50% in 1988, 13% in 1997, and 41% of those expected in 2017 (Zhang et al. 2015). Further, recruitment rates of *Populus* were 41% of expected in 1977, 13% in 1988, 3% in 1997, and 40% of expected in 2017 (Zhang et al. 2015). However, the inequality in rates between GLR and region-wide is underestimated because 66% of *Picea* and 28% of *Populus* recruited 1997–2017 were dead at the time of their measurement. The failure of recruited stems to survive means that the successful recruitment rate for the GLR stand is lower than the total recruitment reported in the results.

Normally, we would expect stands in the southern boreal forest to progress from an overstory of shade-intolerant *Populus* and *Betula* to shade-tolerant *Picea*, although considerable variation is possible (Chen and Popadiouk 2002, Brassard and Chen 2006, Bergeron et al. 2014). Current conceptual models of succession for the

western boreal forest, and Alberta-specifically, lack a shrub-less, low-density woodland phase or bark beetles as a disturbance agent (Chen and Popadiouk 2002). The extremely low rate of successful recruitment over the previous 30 yr means that a new cohort, if one begins, will take decades to structurally replace the rapidly dying overstory. Results from our study suggest that historical successional pathways have been stymied and could be a new normal for other stands in this ecotone, particularly if the bark beetle species seen in our stand outbreak and encroach into regional stands. The recent, widespread die-off of *Populus* across the region has been documented (Michaelian et al. 2011) and the defoliation years (1979–1988) within the GLR match years of outbreaks of *M. disstria* across Alberta (Hogg et al. 2002a). Multiple years of defoliation can cause high mortality (Moulinier et al. 2014) and long-term changes in cell-fibers with possible negative implications for structure and drought response (Hillabrand et al. 2019). The trees used to reconstruct the history of defoliation in the GLR were the surviving, non-rotten cohort, and it is possible that the *Populus* that died before 2017 suffered additional defoliation events or died as a direct result of defoliation. The decline of *Populus* overlaps the continuing drought-related decline of *Picea* growth within the region (Hogg et al. 2017). In addition to being implicated in the depressed *Picea* growth, the extreme 2002 drought was likely associated with the outbreak of bark beetles. Previous research has linked outbreaks of *Dendroctonus rufipennis* to drought (Berg et al. 2006) with warming temperatures hastening generation time (Hansen et al. 2001) and increasing the likelihood of outbreak (Hansen and Bentz 2003). Predictably, the initial beetle outbreak at the GLR plot, in 2002, occurred during the driest year since stand establishment in the 1920s. We speculate that the weakened *Picea* were unable to mount an effective defense against bark beetles, and that this led to the expansion and outbreak within the stand. The combined effects of bark beetles and the severe droughts of recent decades likely stressed *Picea* and resulted in precipitous declines in density, growth, recruitment, and biomass. The confluence of these disturbances seems to have shunted the GLR stand onto a new

trajectory. The dramatic changes seen in forest composition and structure could be a preview for stands across the southwestern boreal forest of Canada. Further studies are needed to test the generality of the demographic patterns we observed in the GLR plot.

Seasonal climate analysis

Precipitation was greatly correlated with tree ring growth for all four of the GLR species. All species were positively correlated with wetter growing seasons and some portion of climate variables in the previous year. This supports the other evidence from the plot showing drought-caused declines in growth in all species and the multi-year influence of climate on tree ring growth. *Picea* in our study showed strong correlations with precipitation in contrast to work by Goldblum and Rigg (2005) in Ontario, who found no correlation with precipitation and *Picea* growth. This discrepancy is possibly due to the local topography of the GLR or regional differences in climate between the southern boreal forest of Alberta and Ontario. The *Populus* in the GLR had high series intercorrelation and tree ring sensitivity but the lowest correlation coefficients of the four-tree species. One explanation is that the repeated insect defoliation obscures growth–climate relationships (see Hogg et al. 2013). However, Huang et al. (2010) also found that *Populus* in Ontario was the least responsive species to recent warming along the southern boreal ecotone. This suggests that *Populus* may be less responsive to climate than its neighboring species.

Pinus was the only species to respond favorably to increasing temperature. It is likely that *Pinus* is temperature-limited within the stand during non-drought years and that warmer temperatures are associated with increased photosynthesis or a longer growing season. Other studies in the Canadian boreal forest have also seen *Pinus* respond favorably with warmer and wetter growing seasons (Brooks et al. 1998, Huang et al. 2010). Cumulatively, the seasonal analysis shows a favorable growth response to growing season precipitation and a largely negative relationship with warming temperatures. If future climates bring warmer growing season temperatures, we predict a decline in *Picea*, *Populus*, and *Betula* ring

growth and a potential increase in *Pinus* growth.

CONCLUSION

We present evidence suggesting that in response to recent drought and warming, a novel successional pathway has developed in at least some stands along the southern edge of the western Canadian boreal forest. A decline in forest vital rates and insect-associated mortality has set the stand on a path toward a state characterized by a continued decline of the original establishing cohort and absent new recruitment. Future droughts could see bark beetles and other insects outbreak in stands in the region. As warming and severe climatic events are expected to continue or increase (Differbaugh and Field 2013), we anticipate that the results presented here may become commonplace throughout the southwestern boreal forest, but this hypothesis requires further testing. Our study highlights the reality that novel disturbance regimes may become widespread across the region and lead to changes in vegetation type. Further, our study highlights the utility of tree-ring analysis when paired with long-term demographic and spatial plots (sensu Lutz 2015). Our use of tree-ring analysis reconstructed the inter-census history of the stand and, paired with the census data, allowed us to identify key events that altered forest density. While our study is novel, several limitations exist. The coarse, decadal interval prevents us from identifying specific years for mortality or recruitment events. Further, the mortality agents we identified may have only been the final agent in a suite of stressors that predisposed the tree to death. Larger, replicated plots with more frequent census intervals would address many of these limitations in future studies and detect change across the region. Other studies (Brassard and Chen 2006, Michaelian et al. 2011, Bergeron et al. 2014, Chen and Luo 2015, Zhang et al. 2015, Gendreau-Berthiaume et al. 2016) have captured broad swathes of demographic and spatial change within the aspen parkland and boreal forest; however, our study elucidates the long-term development of a forest undergoing succession under the influence of pronounced and, in some cases, novel disturbances. Continued monitoring and establishment of new long-term plots will

aid in highlighting continued change and trends within the Canadian boreal forest.

ACKNOWLEDGMENTS

We acknowledge Jerry Shaw for digitization and data management of the original data. Marc La Flèche, Paul Metzler, Evan Fellrath, Joshua Wasyliw, Chloe Christenson, and Dana Hopfauf assisted with stem mapping in 2017. Lee Foote granted access to the GLR Plot in the University of Alberta Botanical Gardens. Funding was provided by the Alberta Conservation Association Grants for Biodiversity to Joseph Birch, and a Natural Sciences and Engineering Research Council of Canada Discovery Grant to Justine Karst.

LITERATURE CITED

- Alberta Biodiversity Monitoring Institute (ABMI). 2018. ABMI Trees & Snags (5342138678144103563) database: Rotation 2. <http://www.ABMI.ca>
- Allen, C. D., et al. 2010. A global overview of drought and heat-induced tree mortality reveals emerging climate change risks for forests. *Forest Ecology and Management* 259:660–684.
- Barber, V., G. Patrick, and B. Finney. 2000. Reduced growth of Alaskan white spruce in the twentieth century from temperature-induced drought stress. *Nature* 405:668–673.
- Berg, E. E., J. David Henry, C. L. Fastie, A. D. De Volder, and S. M. Matsuoka. 2006. Spruce beetle outbreaks on the Kenai Peninsula, Alaska, and Klunane National Park and Reserve, Yukon Territory: relationship to summer temperatures and regional differences in disturbance regimes. *Forest Ecology and Management* 227:219–232.
- Bergeron, Y., H. Y. H. Chen, N. C. Kenkel, A. L. Leduc, and S. E. Macdonald. 2014. Boreal mixedwood stand dynamics: ecological processes underlying multiple pathways. *Forestry Chronicle* 90:202–213.
- Brassard, B. W., and H. Y. H. Chen. 2006. Stand structural dynamics of North American boreal forests. *Critical Reviews in Plant Sciences* 25:115–137.
- Brooks, J. R., L. B. Flanagan, and J. R. Ehleringer. 1998. Responses of boreal conifers to climate fluctuations: indications from tree-ring widths and carbon isotope analyses. *Canadian Journal of Forest Research* 28:524–533.
- Bunn, A., M. Korpela, F. Biondi, F. Campelo, P. Mérian, F. Qeadan, and C. Zang. 2017. dplR: Dendrochronology Program Library in R.
- Chen, H. Y. H., and Y. Luo. 2015. Net aboveground biomass declines of four major forest types with forest ageing and climate change in western Canada's boreal forests. *Global Change Biology* 21:3675–3684.
- Chen, H. Y., and R. V. Popadiouk. 2002. Dynamics of North American boreal mixedwoods. *Environmental Reviews* 10:137–166.
- Cook, E. R. 1985. A Time-series analysis approach to tree ring standardization. Dissertation. University of Arizona, Tucson, Arizona, USA.
- DeRose, R. J., M. F. Bekker, and J. N. Long. 2017. Traumatic resin ducts as indicators of bark beetle outbreaks. *Canadian Journal of Forest Research* 47:1168–1174.
- Dietze, M. C., and P. R. Moorcroft. 2011. Tree mortality in the eastern and central United States: patterns and drivers. *Global Change Biology* 17:3312–3326.
- Diffenbaugh, N. S., and C. B. Field. 2013. Changes in ecologically critical terrestrial climate conditions. *Science* 341:486–492.
- Environment and Climate Change Canada. 2017. Historical climate database: climate stations 3012205 and 3012216 concatenated, 1961 to 2017. http://climate.weather.gc.ca/historical_data/search_historic_data_e.html
- Flora of North America Editorial Committee, editor. 1993. *Flora of North America North of Mexico*. Flora of North America Editorial Committee, Oxford, UK.
- Frellich, L. E., and P. B. Reich. 2010. Will environmental changes reinforce the impact of global warming on the prairie–forest border of central North America? *Frontiers in Ecology and the Environment* 8:371–378.
- Fritts, H. C. 1976. *Tree rings and climate*. Academic Press, London, UK; New York, New York, USA.
- Gendreau-Berthiaume, B., S. E. Macdonald, and J. J. Stadt. 2016. Extended density-dependent mortality in mature conifer forests: causes and implications for ecosystem management. *Ecological Applications* 26:1486–1502.
- Goldblum, D., and L. S. Rigg. 2005. Tree growth response to climate change at the deciduous-boreal forest ecotone, Ontario, Canada. *Canadian Journal of Forest Research* 35:2709–2718.
- Goslee, S. C., and D. L. Urban. 2007. The ecodist package for dissimilarity-based analysis of ecological data. *Journal of Statistical Software* 22:1–19.
- Gray, L. K., and A. Hamann. 2011. Strategies for reforestation under uncertain future climates: guidelines for Alberta. *Canada. PLoS ONE* 6:e22977.
- Hansen, E. M., and B. J. Bentz. 2003. Comparison of reproductive capacity among univoltine, semi-voltine, and re-emerged parent spruce beetles (Coleoptera: Scolytidae). *Canadian Entomologist* 135:697–712.

- Hansen, E. M., B. J. Bentz, and D. L. Turner. 2001. Temperature-based model for predicting univoltine brood proportions in spruce beetle (Coleoptera: Scolytidae). *Canadian Entomologist* 133:827–841.
- Hillabrand, R. M., V. J. Lieffers, E. H. Hogg, E. Martínez-Sancho, A. Menzel, and U. G. Hacke. 2019. Functional xylem anatomy of aspen exhibits greater change due to insect defoliation than to drought. *Tree Physiology* 39:45–54.
- Hogg, E. H., A. G. Barr, and T. A. Black. 2013. A simple soil moisture index for representing multi-year drought impacts on aspen productivity in the western Canadian interior. *Agricultural and Forest Meteorology* 178–179:173–182.
- Hogg, E. H., J. P. Brandt, and B. Kochtubajda. 2002a. Growth and dieback of aspen forests in northwestern Alberta, Canada, in relation to climate and insects. *Canadian Journal of Forest Research* 32:823–832.
- Hogg, E. H., M. Hart, and V. J. Lieffers. 2002b. White tree rings formed in trembling aspen saplings following experimental defoliation. *Canadian Journal of Forest Research* 32:1929–1934.
- Hogg, E. H., and P. A. Hurdle. 1995. The aspen parkland in western Canada: A dry-climate analogue for the future boreal forest? *Water, Air, and Soil Pollution* 82:391–400.
- Hogg, E. H., M. Michaelian, T. I. Hook, and M. E. Undershultz. 2017. Recent climatic drying leads to age-independent growth reductions of white spruce stands in western Canada. *Global Change Biology* 23:5297–5308.
- Holmes, R. L. 1983. Computer-assisted quality control in tree-ring dating and measurement. *Tree-Ring Bulletin* 43:69–78.
- Huang, J., J. C. Tardif, Y. Bergeron, B. Denneker, F. Berninger, and M. P. Girardin. 2010. Radial growth response of four dominant boreal tree species to climate along a latitudinal gradient in the eastern Canadian boreal forest. *Global Change Biology* 16:711–731.
- Kobe, R. K. 1996. Intraspecific variation in sapling mortality and growth predicts geographic variation in forest composition. *Ecological Monographs* 66:181–201.
- Larsson, L. Å. 2018. Coorecorder. Cybis Elektronik & Data AB, Saltsjobaden, Sweden.
- Lutz, J. A. 2015. The evolution of long-term data for forestry: large temperate research plots in an era of global change. *Northwest Science* 89:255–269.
- Meko, D. M., R. Touchan, and K. J. Anchukaitis. 2011. Seascorr: A MATLAB program for identifying the seasonal climate signal in an annual tree-ring time series. *Computers & Geosciences* 37:1234–1241.
- Michaelian, M., E. H. Hogg, R. J. Hall, and E. Arsenault. 2011. Massive mortality of aspen following severe drought along the southern edge of the Canadian boreal forest: aspen mortality following severe drought. *Global Change Biology* 17:2084–2094.
- Moulinier, J., F. Lorenzetti, and Y. Bergeron. 2014. Growth and mortality of trembling aspen (*Populus tremuloides*) in response to artificial defoliation. *Acta Oecologica* 55:104–112.
- Oksanen, J., F. G. Blanchet, R. Kindt, P. Legendre, P. R. Minchin, R. B. O'hara, G. L. Simpson, P. Solyomos, M. H. Stevens, and H. Wagner. 2018. vegan: Community ecology package. R package version 2.5–2.
- Peng, C., Z. Ma, X. Lei, Q. Zhu, H. Chen, W. Wang, S. Liu, W. Li, X. Fang, and X. Zhou. 2011. A drought-induced pervasive increase in tree mortality across Canada's boreal forests. *Nature Climate Change* 1:467–471.
- Percival, D. B., and W. L. B. Constantine. 2006. Exact simulation of Gaussian time series from nonparametric spectral estimates with application to bootstrapping. *Statistics and Computing* 16:25–35.
- R Core Team. 2018. R: A language and environment for statistical computing. R Foundation for Statistical Computing, Vienna, Austria.
- Scheffer, M., M. Hirota, M. Holmgren, E. H. Van Nes, and F. S. Chapin. 2012. Thresholds for boreal biome transitions. *Proceedings of the National Academy of Sciences* 109:21384–21389.
- Soja, A. J., N. M. Tchebakova, N. H. French, M. D. Flannigan, H. H. Shugart, B. J. Stocks, A. I. Sukhinin, E. I. Parfenova, F. S. Chapin III, and P. W. Stackhouse Jr. 2007. Climate-induced boreal forest change: predictions versus current observations. *Global and Planetary Change* 56:274–296.
- Speer, J. H. 2010. Fundamentals of tree-ring research. University of Arizona Press, Tucson, Arizona, USA.
- Stokes, M., and T. Smiley. 1996. An introduction to tree-ring dating. University of Arizona Press, Tucson, Arizona, USA.
- Ung, C.-H., P. Bernier, and X.-J. Guo. 2008. Canadian national biomass equations: new parameter estimates that include British Columbia data. *Canadian Journal of Forest Research* 38:1123–1132.
- van Mantgem, P. J., et al. 2009. Widespread increase of tree mortality rates in the western United States. *Science* 323:521–524.
- Worrall, J. J., G. E. Rehfeldt, A. Hamann, E. H. Hogg, S. B. Marchetti, M. Michaelian, and L. K. Gray. 2013. Recent declines of *Populus tremuloides* in

- North America linked to climate. *Forest Ecology and Management* 299:35–51.
- Zang, C., and F. Biondi. 2015. treeclim: an R package for the numerical calibration of proxy- climate relationships. *Ecography* 38:431–436.
- Zhang, J., S. Huang, and F. He. 2015. Half-century evidence from western Canada shows forest dynamics are primarily driven by competition followed by climate. *Proceedings of the National Academy of Sciences* 112:4009–4014.

SUPPORTING INFORMATION

Additional Supporting Information may be found online at: <http://onlinelibrary.wiley.com/doi/10.1002/ecs2.2698/full>